Oxidization Characterization of Hafnium-Based Ceramics Fabricated by Hot Pressing and Electric Field-Assisted Sintering

Matt Gasch and Sylvia Johnson - NASA Ames Research Center, Moffett Field, CA 94035
Jochen Marschall - SRI International, Menlo Park, CA 94025

Introduction

Ceramic borides, such as hafnium diboride (HfB_2) and zirconium diboride (ZrB_2), are members of a family of materials with extremely high melting temperatures referred to as Ultra High Temperature Ceramics (UHTCs). UHTCs constitute a class of promising materials for use in high temperature applications, such as sharp leading edges on future-generation hypersonic flight vehicles, because of their high melting points.[1]

The controlled development of microstructure has become important to the processing of UHTCs, with the prospect of improving their mechanical and thermal properties.[2-5] The improved oxidation resistance of HfB_2 has also become important if this material is to be successfully used at temperatures above 2000°C. Furthermore, the use of UHTCs on the leading edges of vehicles traveling at hypersonic speeds will mean exposure to a mixed oxidation environment comprised of both molecular and atomic oxygen.

The current study has investigated the high-temperature oxidation behavior of HfB_2-based materials in a pure O_2 environment, as well as in environments containing different levels of dissociated oxygen (O/O_2). Materials were processed by two techniques: conventional hot pressing (HP) and electric field-assisted sintering (FAS). Their oxidation behavior was evaluated in both a tube furnace at 1250°C for 3 hours and in a simulated re-entry environment in the Advanced Heating Facility (AHF) arcjet at NASA Ames Research Center, during a 10-minute exposure to a cold wall heat flux of 250W/cm^2 and stagnation pressure of 0.1-0.2 atm. The microstructure of the different materials was characterized before and after oxidation using scanning electron microscopy (SEM).

Experimental

The raw diboride and carbide powders used in this work were -325 mesh HfB_2 and 1-2μm SiC, both from H.C. Starck Inc. The powders were weighed and combined into a 80%HfB_2 -20%SiC powder mixture by volume, which was then wet-milled with WC(Co) milling media in a planetary mill (Fritsch Pulverisette 5, Germany). The milled powders were carefully dried to prevent phase segregation between the HfB_2 (ρ = 11.12 g/cm^3) and the SiC (ρ = 3.2 g/cm^3).

Hot pressing was conducted at NASA in a graphite element resistance furnace (Thermal Technologies HP50-7010G, Santa Rosa, CA) with vacuum levels of < 200 mTorr. The dried powders were loaded into a 25 mm diameter graphite die lined with Grafoil®. Above 1600 °C, the partial pressure of carbon in the furnace increased significantly and degraded the vacuum. Consequently, the furnace was back-filled with one atmosphere of inert gas (argon or helium), to preserve the graphite element and insulation. Typical sintering conditions required for densification by HP were 1900–2200°C for 1 hour at 25 MPa. [The partial pressure of carbon should be independent of argon whether its 1 atm or 1000 atm.

Field-assisted sintering was performed at the Air Force Research Laboratory (AFRL) at Wright Patterson Air Force Base labs in Dayton, OH using an FCT System GmbH Model HPD 25-1 (Rauenstein, Germany) using the same milled powders as those densified by conventional HP. Samples were again loaded into a 25 mm diameter graphite die lined with Grafoil®. Typical conditions required for FAS densification were 1800–1900°C, with hold times of 5–10 minutes at 20 MPa. Ramp rates used during FAS ranged from 100–300°C per minute. Sample temperature was measured by an optical pyrometer focused on the bottom of a bore hole in the punch ~ 5 mm from the powder.

Details of the manufacture of pure HfB_2 by FAS are presented elsewhere.[6] Essentially, about 15 g of stoichiometric amounts of elemental boron (-325 mesh, Alpha Aesar) and hafnium (-325 mesh, Cerac) powders were mixed in an agate mortar before introduction into a graphite die having an internal diameter of 19 mm and a length of 38 mm. Samples were then reactively sintered using FAS at the University of California Davis.

The density of the consolidated billets and test specimens was measured using the Archimedes method. After the samples were cross-sectioned and polished to a 1-μm finish, the microstructure of consolidated samples was characterized using scanning electron microscopy (FEI ESEM 30, Hillsborough, OR) with accompanying energy dispersive X-ray (EDX) analysis. Grain size analysis was performed using the lineal intercept method without grain shape corrections; no distinction was made between HfB_2 and SiC grains.

Laboratory oxidation studies were performed at SRI International using a furnace-heated quartz flow tube coupled to a 6-kW microwave discharge. UHTC samples (2x2x1 mm) were oxidized at 1250°C for 3 hours in a flowing gas mixture of O_2/13%Ar, with or without the discharge activated. Furnace heating and cooling was done under pure Ar flows. Activation of the microwave discharge converted ~10 percent of the O_2 to atomic oxygen. The total gas pressure was maintained at 3 Torr and the bulk gas velocity was >10 m/s.

Oxidation resistance was also investigated on machined flat-face models in a simulated re-entry environment created via the NASA Ames AHF arcjet. A photo of an as-machined flat-face arcjet model is shown in Figure 1. The model is 25.4 mm in diameter, and the overall height is 8mm. The notch in the stem of the model, shown in the lower left of Figure 1, is used to pin the model into the holder. Models were placed in SiC-coated graphite holders (shown in the center image of the same figure), enabling test durations in excess of 10 minutes. Models and holders were then attached to a water-cooled sting arm that moved the models in and out of the plasma stream (right most image in Figure 1.)

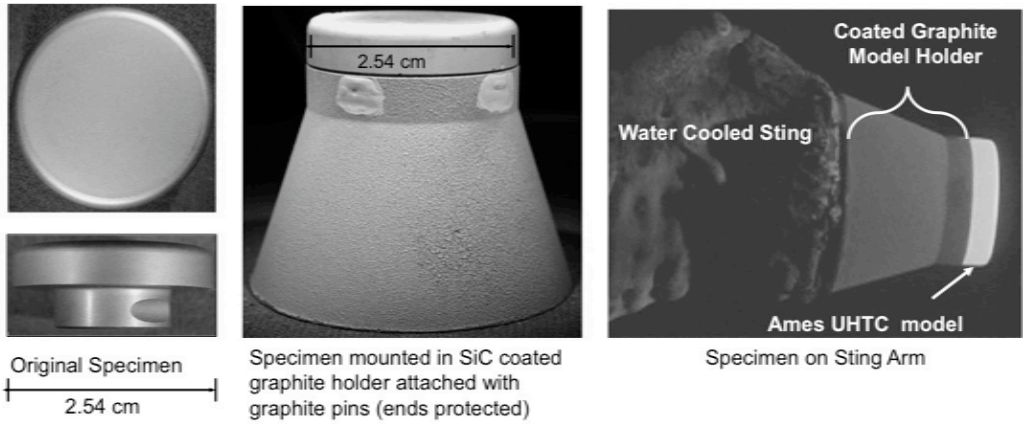

Figure 1. Flat-face arcjet model shown as fabricated, attached to SiC coated graphite holder, and attached to water-cooled sting arm.

A variety of instrumentation was used to calibrate arcjet conditions and measure the thermal response of the materials. Models were tested at a cold wall heat flux of 250 W/cm^2 and a stagnation pressure of 0.1 atm for 10 minutes. At these conditions all of the molecular oxygen was dissociated. Cold wall heat flux values were measured using a copper Gardon gauge and are referenced to a 76 mm diameter hemisphere. However, hot wall heat flux values at the model's surface differ (and are generally lower), because of differences in model geometry, surface temperature, and catalytic efficiency between the water-cooled copper Gardon gauge and the hot oxidizing UHTC surface. (Detailed discussion of the heat flux at the surface of the model is beyond the scope of this work.) Two-color optical pyrometers were used to make surface temperature measurements during the tests.

Post-test furnace and arcjet specimens were cross-sectioned, polished to a 1-μm finish and then inspected by SEM as described above. Oxide thickness was determined by averaging 5-8 thickness measurements across an SEM image. For the arcjet specimens SEM images were taken at the center of the model (12mm from either edge).

Results and Discussion

Processing and Properties

Table 1 lists the physical characteristics of the consolidated samples. The densities of consolidated samples ranged from 95–99% of the theoretical density (TD) computed from the volume fractions and densities of the individual compounds.

Table 1. Summary of physical characterizations done on consolidated samples investigated in this study.

Sample ID	Density g/cm^3	Grain Size μm
Pure HfB_2 (FAS)	10.7 (95% TD)	4.0
HfB_2-20SiC (HP)	9.5 (99% TD)	7.7
HfB_2-20SiC (FAS)	9.5 (99% TD)	4.1

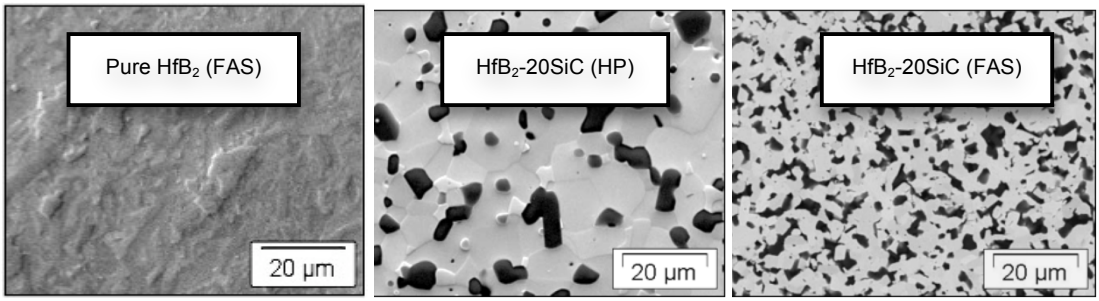

Figure 2. SEM images of the UHTC samples comparing the differences in microstructure between hot pressing and field assisted sintering.

Figure 2 shows SEM micrographs of polished sections the three different materials investigated in this study. In the composite materials, the dark phase in the images is SiC and the lighter phase is HfB_2. While both HP and FAS produced HfB_2-20SiC composites close to full density, it is evident from these images and the grain sizes reported in Table 1 that FAS results in a finer-grained microstructure than HP.

Oxidation Results

After oxidation, all sample surfaces turned white due to the formation of an oxide layer. Table 2 summarizes the experimental values of measured oxide thicknesses.

Table 2. Summary of the furnace oxidation and arcjet conditions, sample temperature and post-test oxide thickness of cross-sectioned samples.

Sample ID	Sintering Method	Test Method	Pressure atm	Test Duration min	Surf Temp °C	Environment	Oxide Thickness μm
Pure HfB_2	FAS	Furnace	0.004	180	1250	O_2	13.6
Pure HfB_2	FAS	Furnace	0.004	180	1250	O/O_2	25.1
HfB_2-20SiC	HP	Furnace	0.004	180	1250	O_2	8.7
HfB_2-20SiC	HP	Furnace	0.004	180	1250	O/O_2	10.3
HfB_2-20SiC	FAS	Furnace	0.004	180	1250	O_2	8.5
HfB_2-20SiC	FAS	Furnace	0.004	180	1250	O/O_2	9.0
HfB_2-20SiC	HP	Arcjet	0.20	10	1690	O	13.0
HfB_2-20SiC	FAS	Arcjet	0.10	10	1530	O	3.1

The pure HfB_2 material formed a thick 13.6 μm HfO_2 surface layer under molecular oxygen. However, when subjected to a partially-dissociated oxygen flow, HfB_2 oxidized even more readily, forming a 25.1 μm thick oxide layer under the same temperature-pressure-time conditions, an increase of ~85%, as shown in Figure 3. Thus, even a relatively small level of oxygen dissociation can exert a strong influence on the oxidation of pure HfB_2.

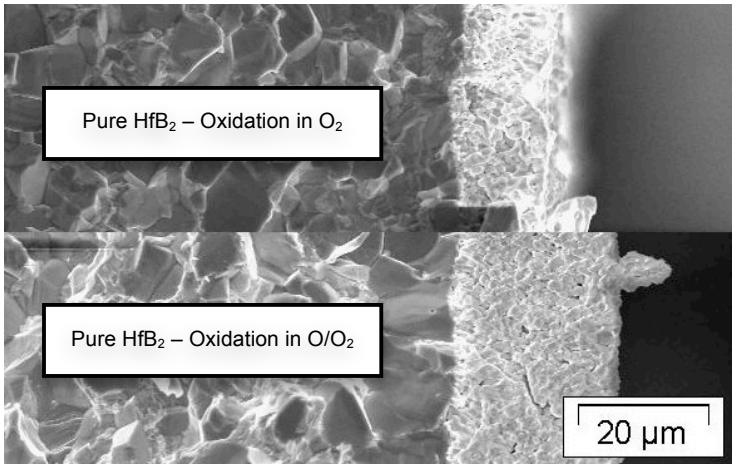

Figure 3. SEM images of the pure HfB_2 furnace oxidized in O_2 and in an O/O_2 environment.

The addition of SiC to HfB_2 decreased the measured oxide thicknesses of both HP and FAS processed materials in the furnace tests. Under molecular oxygen flow this decrease was approximately 40% and under partially-dissociated oxygen flow approximately 60%, demonstrating that SiO_2 formation is beneficial for the protection of HfB_2 in both molecular and partially-dissociated oxygen environments. The oxide layer formed on HfB_2-20SiC materials in a partially-dissociated oxygen flow was moderately larger than under molecular oxygen flow, about 6% thicker for the FAS material and about 18% thicker for the HP material, so the influence of atomic oxygen is still present, although not as strong as for pure HfB_2.

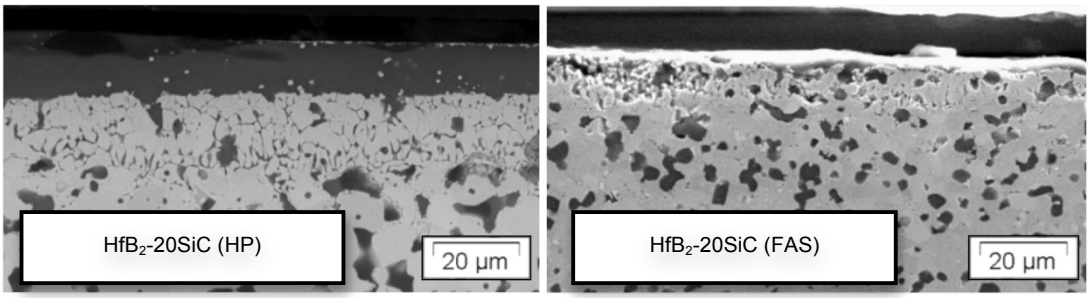

Figure 4. SEM images of the arcjet tested HfB_2-SiC samples comparing the differences in oxide thickness between HP and FAS processed material.

Interestingly, the HfB_2-20SiC samples processed by FAS showed thinner oxide thickness values, compared to the HP samples, particularly under the partially-dissociated oxygen flow. Since the atomic oxygen concentration in the furnace experiments is small, it is of interest to investigate if this trend is maintained at higher O-atom densities. Therefore, HfB_2-SiC samples processed by both HP and FAS were subjected to an arcjet oxidation test, wherein the flow of oxygen was 100% dissociated. SEM images of the post-test arcjet models are shown in Figure 4. After arcjet testing, the difference in oxide thickness between the HP material and the FAS material was even more pronounced than after the furnace

oxidation experiments; the HP sample had an average oxide thickness ~300% greater than the FAS sample.

Hwang et al.[7-8] recently reported that the incorporation of nano-sized SiC particles improved the oxidation resistance of hot pressed ZrB_2 ceramics. They proposed that ceramics with reduced grain size (the SiC phase in particular) have an increased diboride/SiC interface length per unit area of exposed surface and a decreased spacing between Si-containing particles. The decrease in spacing between SiC particles allows the surface to more rapidly form a protective oxide over the diboride phase. The results of our work appear to support this hypothesis; the presence of a SiC phase with very refined grain size improves oxidation resistance in both molecular and dissociated oxygen environments.

Conclusions

The current study has investigated the oxidation behavior of pure $HfB_2$and HfB_2-SiC materials in a molecular oxygen environment as well as in an environment with dissociated oxygen (O/O_2). Materials were processed by two techniques; conventional hot pressing as well as electric field-assisted sintering. The pure HfB_2 material formed a thick HfO_2 scale under O_2. However, when subjected to a partially-dissociated oxygen flow, HfB_2 oxidized more readily and the oxide thickness increased an average of 85%. The addition of SiC to HfB_2 decreased measured oxide thicknesses of HP and FAS processed materials tested in flowing O_2 by approximately 40% due to the formation of a protective SiO_2 layer. In partially-dissociated oxygen, HfB_2-20SiC samples only saw oxide thickness increase an average of 6-18% due to the protective nature of SiO_2 over the HfB_2 phase. The samples processed by FAS showed thinner oxides than the HP samples, when exposed in an identical manner to O_2, O/O_2, and O oxidizing environments. This observed behavior was attributed to a decrease in spacing between SiC particles and increased diboride/SiC interface length per unit area of exposed surface which is believed to allow the surface to more rapidly form a protective oxide over the diboride phase.

Acknowledgements

This work was funded by the Hypersonics element of the Fundamental Aeronautics Program at NASA Aeronautics Research Mission Directorate (ARMD). J. Marschall acknowledges the support of the High-Temperature Aerospace Materials Program of the Air Force Office of Scientific Research through contracts FA9550-050-C-0020 and FA9550-08-C-0049. We also acknowledge NASA-SCAP for their critical financial support of the arcjet operational capability at Ames.

References

1. L. Kaufman and, E.V. Clougherty, 1963, RTD-TRD-N69-73497Part XXXVII, ManLabs Inc., Cambridge, MA.
2. D-W Ni, G-J. Zhang, Y-M. Kan and Y. Sakka, 2009,Scripat Mat., 60, 913-916.
3. F. Monteverde, Composites Sci. and Tech., 2005, 65, 1869-1879.
4. L. Chen, Y.Gu, L. Shi, Z. Yang, J. Ma and J. Qian, J. of Alloys and Comp., 2004, 36, 8353-356.
5. X. Zhang, Xu, L., Du, S., Han, W., Han, J., Scripta Mat., 2008, 59, 1222-1225.
6. U. Anselmi-Tamburini, Y. Kodera, M. Gasch, C. Unuvar, Z.A. Munir, M. Ohyanagi and S.M. Johnson, J. Mat. Sci., 2006, 41, 3097–3104.
7. S.S. Hwang, A.L. Vasiliev and N.P. Padture, Mat. Sci. Eng. A, 2007, 464, 216-224.
8. S-Q. Guo, J-M. Yang, D. Tanaka and Y. Kagawa, Composites Sci. and Tech., 2008, 68, 3033-3040.